



Complete visualization using indocyanine green in thoracic surgery for pulmonary sequestration

Keita Nakanishi[^], Yuka Kadomatsu, Harushi Ueno, Taketo Kato, Shota Nakamura, Tetsuya Mizuno, Toyofumi Fengshi Chen-Yoshikawa

Department of Thoracic Surgery, Nagoya University Graduate School of Medicine, Nagoya, Japan

Correspondence to: Keita Nakanishi, MD. Department of Thoracic Surgery, Nagoya University Graduate School of Medicine, 65 Tsurumai-cho, Showa-ku, Nagoya 466-8550, Japan. Email: knakanishi@med.nagoya-u.ac.jp.

Abstract: Preoperative three-dimensional computed tomography (CT) facilitates accurate identification of aberrant systemic arteries in thoracic surgery for pulmonary sequestration (PS). Furthermore, the boundary between normal and sequestered lungs can be visualized using the spread of fluorescent indocyanine green (ICG) when performing surgery for PS. This study aimed to determine how to completely visualize anatomical variations, safely treat aberrant arteries, remove only sequestered lungs, and perform minimally invasive surgery for PS. Seventeen patients underwent lung resection for intralobar PS at our institution between 2009 and 2022. We retrospectively reviewed the surgical outcomes and intraoperative images using ICG to assess the efficacy and feasibility of near-infrared fluorescence imaging. Since 2019, intraoperative near-infrared fluorescence imaging with ICG has been used in six patients, including four females and two males (median age, 56 years), to visualize the boundary between normal and sequestered lungs. Aberrant arteries were identified using preoperative three-dimensional CT, and the boundary between sequestered and normal lungs could be clearly delineated intraoperatively using ICG in all cases. The median operative time was 145 min (range, 88–167 min), and the median blood loss was 5 mL (range, 1–191 mL). The overlay mode using near-infrared thoracoscopy, which merges visible light images with fluorescent images, was safer and more useful than conventional thoracoscopy for delineating boundaries with electrocautery. No intraoperative or postoperative complications occurred. The median postoperative hospital stay was 5 days (range, 3–7 days). Intraoperative identification of the boundary between normal and sequestered lungs using ICG was simple and feasible. We suggested that this technique was effective for lesion resection and normal lung preservation during surgery for intralobar PS.

Keywords: Pulmonary sequestration (PS); surgery; three-dimensional computed tomography (three-dimensional CT); indocyanine green (ICG); visualization

Submitted Jun 02, 2023. Accepted for publication Sep 14, 2023. Published online Oct 10, 2023.

doi: 10.21037/jtd-23-892

View this article at: <https://dx.doi.org/10.21037/jtd-23-892>

Introduction

Pulmonary sequestration (PS) is a rare congenital malformation characterized by nonfunctional lung tissue fed by aberrant systemic arteries (1). Surgical lung resection is commonly recommended for intralobar PS, regardless of the presence or absence of symptoms (2).

Accurate treatment of aberrant arteries and adequate dissection of the sequestered lung are important for intralobar PS surgery. Thus, the complete visualization of perioperative and intraoperative anatomical variations is necessary for minimally invasive surgery to treat PS. We previously reported the usefulness and pitfalls of hybrid

[^] ORCID: 0000-0001-8862-9222.

surgery with preoperative coil embolization for aberrant arteries (3,4). Furthermore, several reports have described the optimal management of aberrant arteries (5,6). However, information regarding how to detect and dissect the boundary between normal and sequestered lungs is scarce.

Various methods for identifying segments have been described, including the intraoperative use of indocyanine green (ICG) (7,8). ICG is widely used in surgery for several organs. In thoracic surgery, the use of ICG has been introduced as a technique to detect organ blood flow (9-11). With advances in fluorescence surgery, visualization of the boundary between normal and sequestered lungs using ICG is now performed for PS surgery (3,12-17). However, most descriptions of the use of ICG to distinguish normal lungs from sequestered lungs were case reports only, and the efficacy and feasibility of the technique have not been fully evaluated.

Therefore, this study aimed to determine how to completely visualize anatomical variations, safely treat aberrant arteries, remove only sequestered lungs, and perform minimally invasive thoracic surgery for PS. We retrospectively reviewed surgical outcomes and intraoperative images in patients with intralobar PS using ICG to assess the efficacy and feasibility of this simple technique. We present this article in accordance with the STROBE reporting checklist (available at <https://jtd.amegroups.com/article/view/10.21037/jtd-23-892/rc>).

Methods

The study was conducted in accordance with the Declaration of Helsinki (as revised in 2013). This study was approved by the Institutional Review Board of Nagoya University Hospital (No. 2020-0375). Individual consent for this retrospective analysis was waived. Seventeen patients underwent lung resection of intralobar PS at Nagoya University Hospital between January 2009 and November 2022, and intraoperative near-infrared fluorescence imaging with ICG was performed in six (35%) of these patients. All intralobar PS cases were diagnosed as Pryce type III based on the findings of preoperative images. Data from institutional databases and patient medical records were retrospectively reviewed to investigate clinical characteristics and surgical outcomes, including age, sex, operative year, smoking history, history of pneumonia, location and size of disease, number of aberrant arteries, maximal size of aberrant arteries,

preoperative interventions, surgical approaches, aberrant artery resection method, operative times, blood loss, and postoperative hospital durations and complications. In cases where ICG was used, intraoperative images were retrospectively analyzed to assess the boundary between normal and sequestered lungs. The Mann-Whitney *U* test and Fisher's exact test were used to compare continuous and categorical variables, respectively, between the groups. For all analyses, *P* values <0.05 were used to denote statistical significance. All statistical analyses were performed using SPSS version 25.0 (IBM Corporation, Armonk, NY, USA).

All patients underwent preoperative contrast-enhanced computed tomography (CT) to confirm the presence and origin of aberrant arteries before surgery for intralobar PS, and three-dimensional images were reconstructed to evaluate aberrant arteries (*Figure 1*). Open thoracotomy was considered if the lesion was large or intense adhesion was expected because of a history of previous thoracic surgery or inflammation. Lobectomy rather than segmentectomy was chosen if the lesion was larger than 50 mm or spanned multiple segments. During surgery, aberrant arteries were first identified and dissected. The optimal treatment of an aberrant artery is controversial; therefore, the method for resecting aberrant arteries was chosen by the surgeons. Furthermore, the veins that drained the sequestered lungs were also dissected. After dissection of the aberrant arteries and veins, an anesthesiologist administered ICG at a dose of 5.0–7.5 mg/body. Next, the boundary between normal and sequestered lungs was identified using the real-time IMAGE 1 S™ D-LIGHT P SCB, RUBINA™ (Karl Storz, Germany) or VISERA ELITE II OTV-S300 (Olympus, Japan) system. When thoracotomy was performed, we performed ICG detection while the lights in the operating room were dimmed and the open chest wound was covered with gauze or sheets. While visualizing this boundary, the dissection line was marked by electrocautery. If ICG was not used, the dissection line was determined macroscopically. Finally, the sequestered lungs were dissected from the normal lungs using a stapler and guided by the marked line.

Results

Table 1 shows the clinical characteristics of the 17 surgical cases with intralobar PS. Six males and 11 females, with a median age of 38 years (range, 16–69 years), were included in this study. Eleven patients (65%) never

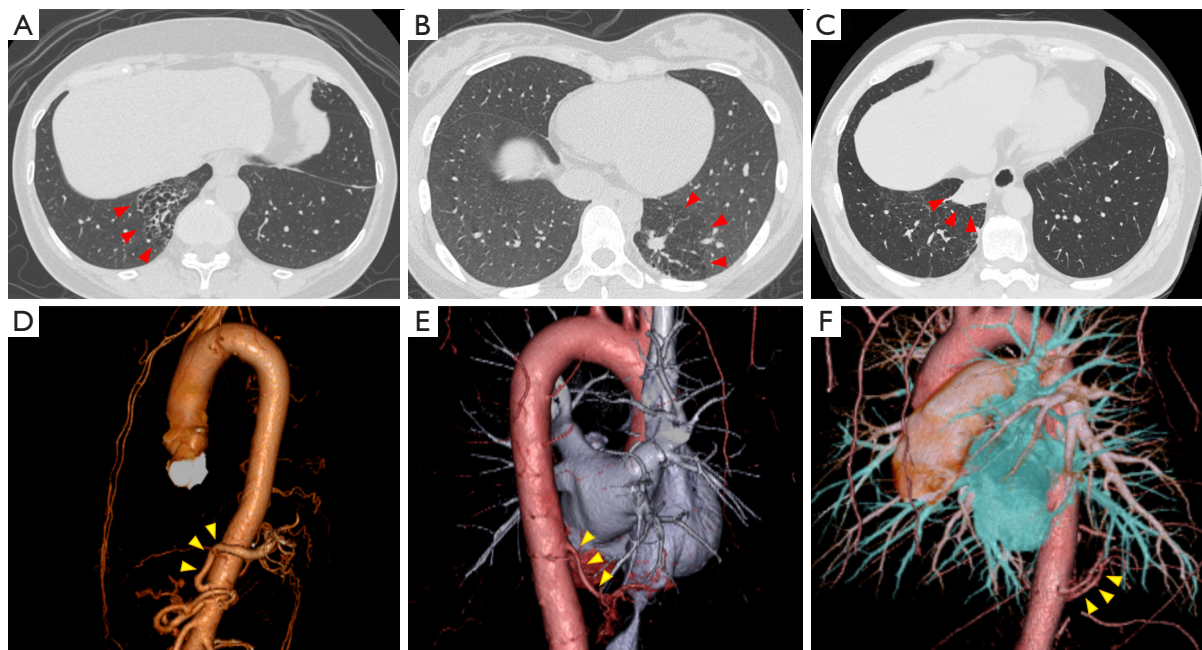


Figure 1 Preoperative computed tomographic images showing intralobar pulmonary sequestration with a mass and cystic lesions (red arrowheads) in cases 2 (A), 3 (B), and 6 (C). Reconstructed three-dimensional images showing the origin and running of aberrant arteries (yellow arrowheads) in cases 1 (D), 4 (E), and 5 (F).

Table 1 Clinical characteristics of surgical cases with intralobar pulmonary sequestration

Characteristics	n=17
Age, years	38 [16–69]
Sex, female	11 [65]
Smoking history, never-smoker	11 [65]
Location	
Right lower lobe	8 [47]
Left lower lobe	9 [53]
Size of disease, mm	49 [25–112]
Preoperative intervention	4 [24]
Surgical approach	
Open thoracotomy	12 [71]
Thoracoscopic surgery	5 [29]
Type of operation	
Lobectomy	6 [35]
Basal segmentectomy	3 [18]
S10 segmentectomy	8 [47]
Operative time, min	159 [88–450]
Blood loss, mL	23 [1–191]
Intraoperative use of ICG	6 [35]

Data are presented as n [%] or median [range]. ICG, indocyanine green.

smoked. Preoperatively, four patients (24%) underwent coil embolization of the aberrant arteries. Lobectomy was performed in six patients (35%), whereas segmentectomy was performed in 11 patients (65%). Although the boundary between normal and sequestered lungs was confirmed visually without the use of ICG in four patients (24%), it was unclear or difficult to judge in the remaining 13 patients. Six patients underwent lung resection using intraoperative ICG to visualize the boundary between normal and sequestered lungs.

The clinical features and surgical outcomes of the six patients who underwent lung resections for intralobar PS using intraoperative ICG are summarized in *Tables 2,3*. All six operations were performed after 2019, and the patients included four females and two males, with a median age of 56 years (range, 16–69 years). Three patients had a history of pneumonia. All patients underwent thoracoscopic segmentectomy, except for case 2, who underwent right upper lobectomy for lung cancer via a thoracotomy performed simultaneously. In case 1, preoperative intervention with coil embolization of an aberrant artery was performed because the vessel was large and originated from the abdominal aorta. Preoperative intervention was also performed in case 2. Aberrant arteries were

Table 2 Clinical features in patients with pulmonary sequestration using intraoperative ICG

Patient	Operative year	Age, years	Sex	Smoking history	History of pneumonia	Method of operation	Origin of aberrant artery	Number of aberrant arteries	Maximal size of aberrant artery, mm
1	2019	56	Female	Never	Yes	VATS, Seg	Abdominal aorta	1	8
2	2020	68	Female	Ex-smoker	No	Open, Seg	Thoracic aorta	1	4
3	2020	16	Female	Never	Yes	VATS, Seg	Thoracic aorta	2	9
4	2021	69	Female	Never	No	VATS, Seg	Thoracic aorta	1	5
5	2021	30	Male	Never	No	VATS, Seg	Thoracic aorta	2	5
6	2022	56	Male	Never	Yes	VATS, Seg	Thoracic aorta	1	2

ICG, indocyanine green; VATS, video-assisted thoracic surgery; Seg, segmentectomy.

Table 3 Surgical outcomes in patients with pulmonary sequestration using intraoperative ICG

Patient	Preoperative intervention	Resection of aberrant artery	Operative time, min	Blood loss, mL	Description of boundary using ICG	Postoperative hospital stays, days	Postoperative complication
1	Yes [†]	Stapler	116	5	Fine	5	None
2	Yes [†]	Ligation	167	191	Fine	7	None
3	None	Ligation	164	32	Fine	4	None
4	None	Ligation + stapler	125	1	Fine	5	None
5	None	Ligation (clip)	88	1	Fine	3	None
6	None	Ligation (clip)	165	5	Fine	5	None

[†], performing embolization of aberrant artery using coils the day before surgery. ICG, indocyanine green.

resected in various ways, including ligation (with clip) and stapling. The median operative time was 145 min (range, 88–167 min), and the median blood loss was 5 mL (range, 1–191 mL). The boundary between the sequestered and normal lungs was clearly visualized in all six cases (*Figure 2*). The overlay mode using near-infrared thoracoscopy, which merges visible light images with fluorescent images, was safer and more useful than conventional thoracoscopy in delineating the demarcation line by electrocautery (*Figure 3*). The sequestered lungs were separated from the normal lungs using a stapler without problems in all six patients; no sequestered lungs were left behind. The pathological examination confirmed that each lesion was completely resected. No intraoperative or postoperative complications occurred. The median postoperative hospital stay was 5 days (range, 3–7 days). No obvious recurrence was observed during follow-up.

The clinical characteristics and surgical outcomes in patients (n=6) for whom ICG was administered were retrospectively compared with those in patients for whom

ICG was not administered (n=11), as shown in *Table 4*. No significant differences in age, sex, smoking history, Brinkman index, history of pneumonia, or location and size of disease were detected between the two groups. The ICG group included significantly more video-assisted thoracic surgeries (83% *vs.* 0%; $P<0.001$) and segmentectomies (100% *vs.* 46%; $P=0.037$) than the non-ICG group. No significant difference in the median operative times was observed between the two groups (144 *vs.* 159 min; $P=0.30$). However, the postoperative hospital stay was significantly shorter in the ICG group than in the non-ICG group (5 *vs.* 7 days; $P=0.037$). Furthermore, we performed additional subgroup analysis to compare patients who underwent segmentectomy using ICG (n=6) with those who underwent segmentectomy without ICG (n=5) (*Table S1*). The ICG group included significantly more video-assisted thoracic surgeries (83% *vs.* 0%; $P=0.015$) than the non-ICG group. The postoperative hospital stay was significantly shorter in the ICG group than in the non-ICG group (5 *vs.* 10 days; $P=0.03$).

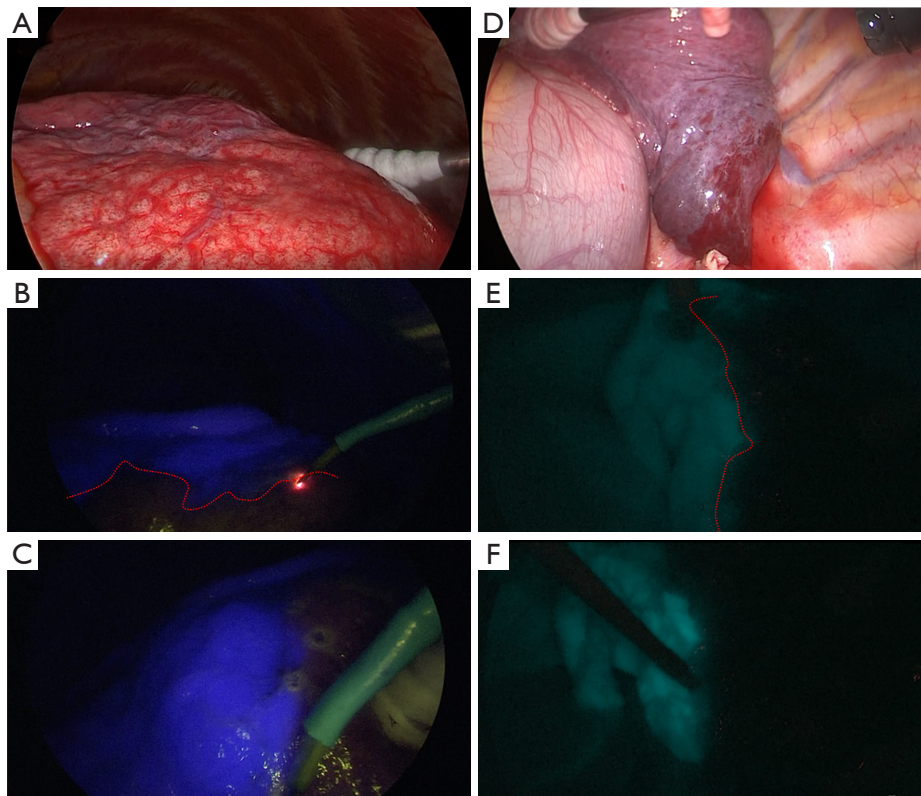


Figure 2 Intraoperative images. Normal visible light image (A); intraoperative identification (B) and marking (C) of the boundary between the normal and sequestered lungs with intravenous ICG using the IMAGE 1 STM D-LIGHT P SCB system (Karl Storz, Germany) in case 1. Normal visible light image (D); intraoperative identification (E) and marking (F) of the boundary between the normal and sequestered lungs by intravenous ICG using the VISERA ELITE II OTV-S300 system (Olympus, Japan) in case 3. Red dotted lines: the visualized boundaries between the normal and sequestered lungs. ICG, indocyanine green.

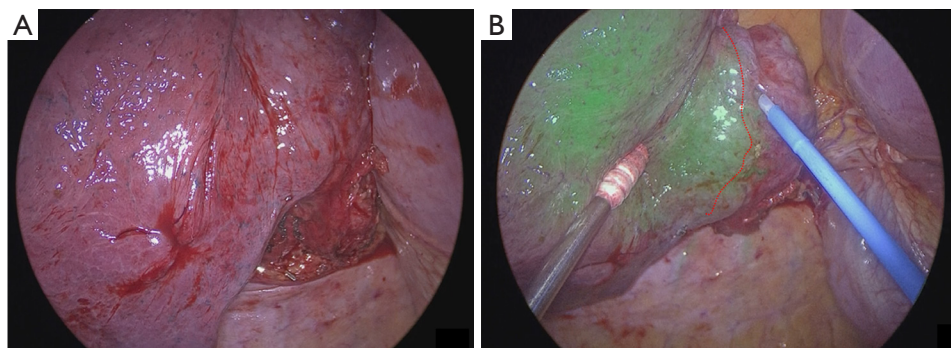


Figure 3 Intraoperative images. Normal visible light image (A); intraoperative identification and marking (B) of the boundary between the normal and sequestered lungs by intravenous ICG using the IMAGE 1 STM RUBINATM system (Karl Storz, Germany) in case 6. Red dotted lines: the visualized boundary between the normal and sequestered lungs. ICG, indocyanine green.

Table 4 Comparison of clinical characteristics and surgical outcomes between patients with and without ICG

Characteristics	ICG group (n=6)	Non-ICG group (n=11)	P value
Age, years	56 [16–69]	34 [28–53]	0.22
Sex			1
Male	2 [33]	4 [36]	
Female	4 [67]	7 [64]	
Smoking history			0.33
Never-smoker	5 [83]	6 [54]	
Ex-smoker	1 [17]	5 [46]	
Brinkman index	0 [0–600]	0 [0–400]	0.53
History of pneumonia	2 [33]	5 [46]	1
Location			1
RLL	3 [50]	5 [46]	
LLL	3 [50]	6 [54]	
Size of disease, mm	45 [25–49]	67 [27–112]	0.062
Approach of operation			<0.001
Open	1 [17]	11 [100]	
VATS	5 [83]	0	
Type of operation			0.037
Segmentectomy	6 [100]	5 [46]	
Lobectomy	0	6 [54]	
Maximal size of aberrant artery, mm	5 [2–9]	5 [2–10]	1
Preoperative intervention	2 [33]	2 [18]	0.58
Operative time, min	144 [88–167]	159 [90–450]	0.3
Blood loss, mL	5 [1–191]	46 [11–183]	0.098
Postoperative hospital stays, days	5 [3–7]	7 [4–11]	0.037

Data are presented as n [%] or median [range]. ICG, indocyanine green; RLL, right lower lobe; LLL, left lower lobe; VATS, video-assisted thoracic surgery.

Discussion

Surgical lung resection is the optimal treatment for intralobar PS, regardless of the presence or absence of symptoms (2). Although lobectomy is performed to ensure complete resection of the sequestered lung, sublobar resection of the sequestered lung is often performed, depending on the size and location, to reduce loss of respiratory function. Sakuma *et al.* suggested that sublobar surgery, including segmentectomy or wedge resection, is useful when the sequestered lung is limited to a segment and when the benign lesion can be completely removed (18).

We perform segmentectomies for intralobar PS at our institution, unless the lesion is larger than 50 mm or is present in multiple segments. For these segmentectomies, the accurate identification of the boundary between the normal and sequestered lungs is crucial. Over-resection can unnecessarily decrease respiratory function, whereas incomplete resection of the sequestered lung may cause disease recurrence. Luján *et al.* reported that cystic lung lesions recurred from the staple line after the resection of congenital cystic adenomatoid malformation and that PS was sometimes associated with congenital cystic

adenomatoid malformation and contained features of both (19). Therefore, the accurate identification of the boundary between the normal and sequestered lungs is essential for the successful resection of intralobar PS. The boundary between normal and sequestered lungs was conventionally identified by direct thoracoscopic visualization or air insufflation. However, the identification of the boundary using ICG and fluorescence imaging has recently been reported (3,12-17). We previously reported a case of thoracoscopic lobectomy using ICG to detect interlobar fissure in a patient with displaced B3 and no fissure (20). Furthermore, Kim *et al.* reported a case of intralobar PS and demonstrated the usefulness of ICG in distinguishing between normal and sequestered lungs in robotic sublobar resection (12). ICG is injected into the peripheral vein after aberrant arteries and veins are resected to visualize the boundary between normal and sequestered lungs under inflated light, according to the degree of blood flow. In this study, the boundary between the sequestered and normal lungs was clearly identified using ICG in all six cases (*Figure 2*). Furthermore, previous reports have demonstrated the usefulness of this simple technique (3,12-17). The successful results of this study may be related to disease-specific features, such as the high prevalence of PS in young nonsmokers. Hypovascularity of the peripheral lung can make visualization of the contour more difficult in some cases, such as severe anthracosis of the lung (7). Furthermore, we retrospectively compared the surgical outcomes in patients with ICG with those in patients without ICG to assess the efficacy of this technique. Although the number of patients in this study was small and the data were preliminary, this is the first report to compare the usefulness of ICG in patients with PS. We demonstrated that the postoperative hospital stay was significantly shorter when ICG was used than when ICG was not administered (5 vs. 7 days; $P=0.037$). However, differences in the approach and types of operations should also be considered. Additionally, we performed subgroup analysis to compare patients who underwent segmentectomy using ICG with those who underwent segmentectomy without the use of ICG (*Table S1*). However, the results of the subgroup analysis were similar to those presented in *Table 4*. We considered that the difference in the surgical approach significantly contributed to the difference in postoperative hospital stays. Moreover, the difference in the surgical approach may majorly depend on the surgical era. Therefore, further investigation of more cases using ICG in the modern era is necessary.

Plane pulmonary intersegmental identification using intraoperative ICG is simple, safe, and inexpensive. However, there are several limitations. First, the intraoperative use of ICG may lead to an allergic reaction. The frequency of severe adverse events, such as anaphylactic shock, is 0.05% (21). In several previous reports, including our experiences, an ICG dose of 5.0–7.5 mg was used (3,4,16,17), whereas doses of 0.1–0.25 mg/kg body weight were used in other studies (12-15). No cases of ICG allergies in patients with PS have been reported. Second, ICG may be washed out rapidly, causing the loss of staining. Misaki *et al.* reported that the area with a normal blood supply was stained within 13 s (range, 8–18 s) and that the maximum staining intensity was attained 28 s (range, 20–33 s) after the injection of ICG in segmentectomy for eight patients (11). However, this problem can be solved by administering ICG multiple times, as long as the patient has no ICG allergies. On the other hand, we should immediately mark considering that ICG may seep into the resected side over time after administration. Another problem highlighted by Matsuura *et al.* is the danger and instability when marking the dissection line with electrocautery because the background is slightly darkened when visualizing only ICG fluorescence (7). We also felt that marking using electrocautery on a dark background risked damage to the lung or other organs (*Figure 2B,2C,2E,2F*). However, the overlay mode, which uses near-infrared thoracoscopy to merge visible light images with fluorescent images, is safe and useful (*Figure 3*). Furthermore, overlay images are feasible and useful in robotic surgery (12), and the expansion of its indication for PS is expected along with the spread of robotic surgery. Finally, near-infrared thoracoscopy systems are expensive, and the equipment is highly specialized. A limitation of our study was the small number of patients, and our analysis might have been underpowered to identify differences in several values in comparisons. Furthermore, follow-up data were inadequate, including postoperative CT images because of benign disease. Thus, we must continue to accumulate and examine patients who undergo surgery for intralobar PS using ICG to determine the efficacy of this technique.

Conclusions

In conclusion, we suggested the efficacy and safety of resecting sequestered lungs using intraoperative ICG fluorescence imaging through a series of cases. Although the technique has several limitations and continuous accumulation and improvement in this technique are

required, ICG fluorescence imaging can be routinely used in surgery for patients with limited intralobar PS lesions.

Acknowledgments

The authors thank Enago (www.enago.jp) for the English language review.

Funding: None.

Footnote

Reporting Checklist: The authors have completed the STROBE reporting checklist. Available at <https://jtd.amegroups.com/article/view/10.21037/jtd-23-892/rc>

Peer Review File: Available at <https://jtd.amegroups.com/article/view/10.21037/jtd-23-892/prf>

Conflicts of Interest: All authors have completed the ICMJE uniform disclosure form (available at <https://jtd.amegroups.com/article/view/10.21037/jtd-23-892/coif>). TFCY serves as an unpaid editorial board member of *Journal of Thoracic Disease* from April 2022 to March 2024. The other authors have no conflicts of interest to declare.

Ethical Statement: The authors are accountable for all aspects of the work in ensuring that questions related to the accuracy or integrity of any part of the work are appropriately investigated and resolved. The study was conducted in accordance with the Declaration of Helsinki (as revised in 2013). This study was approved by the Institutional Review Board of Nagoya University Hospital (No. 2020-0375). Individual consent for this retrospective analysis was waived.

Open Access Statement: This is an Open Access article distributed in accordance with the Creative Commons Attribution-NonCommercial-NoDerivs 4.0 International License (CC BY-NC-ND 4.0), which permits the non-commercial replication and distribution of the article with the strict proviso that no changes or edits are made and the original work is properly cited (including links to both the formal publication through the relevant DOI and the license). See: <https://creativecommons.org/licenses/by-nc-nd/4.0/>.

References

1. Kravitz RM. Congenital malformations of the lung. *Pediatr Clin North Am* 1994;41:453-72.
2. Li XK, Luo J, Wu WJ, et al. Effect of different therapeutic strategies on the clinical outcome of asymptomatic intralobar pulmonary sequestration. *Interact Cardiovasc Thorac Surg* 2019;29:706-13.
3. Hakiri S, Fukui T, Chen-Yoshikawa TF. Combined surgical therapy for pulmonary sequestration and aberrant artery from the abdominal aorta. *Gen Thorac Cardiovasc Surg* 2021;69:1031-4.
4. Nakanishi K, Goto M, Nakamura S, et al. Lessons learned from hybrid surgery with preoperative coil embolization for an aberrant artery in pulmonary sequestration. *Surg Case Rep* 2021;7:192.
5. Leoncini G, Rossi UG, Ferro C, et al. Endovascular treatment of pulmonary sequestration in adults using Amplatzer® vascular plugs. *Interact Cardiovasc Thorac Surg* 2011;12:98-100.
6. Hewett L, Kwon J, Adams JD, et al. Intralobar Pulmonary Sequestration With Aneurysmal Feeding Vessel: Use of Hybrid Surgical Management. *Ann Thorac Surg* 2016;102:e533-5.
7. Matsuura Y, Ichinose J, Nakao M, et al. Recent fluorescence imaging technology applications of indocyanine green in general thoracic surgery. *Surg Today* 2020;50:1332-42.
8. Okada M, Mimura T, Ikegaki J, et al. A novel video-assisted anatomic segmentectomy technique: selective segmental inflation via bronchofiberoptic jet followed by cautery cutting. *J Thorac Cardiovasc Surg* 2007;133:753-8.
9. Nakamura S, Goto M, Chen-Yoshikawa TF. Fluorescence-guided thoracic surgery. *J Vis Surg* 2021;7:18.
10. Chen-Yoshikawa TF, Fukui T, Nakamura S, et al. Current trends in thoracic surgery. *Nagoya J Med Sci* 2020;82:161-74.
11. Misaki N, Chang SS, Igai H, et al. New clinically applicable method for visualizing adjacent lung segments using an infrared thoracoscopy system. *J Thorac Cardiovasc Surg* 2010;140:752-6.
12. Kim WD, Wei B. Robotic resection of pulmonary sequestration with fluorescence image guidance. *Ann Thorac Surg* 2022;115:e15-6.
13. Koike S, Miyazawa M, Kobayashi N. Thoracoscopic resection of pulmonary sequestration with carbon dioxide insufflation and indocyanine green. *Interact Cardiovasc Thorac Surg* 2022;35:ivac209.
14. Lian KH, Lin MW. Indocyanine green imaging to identify intralobar pulmonary sequestration for uniportal thoracoscopic resection. *J Minim Access Surg*

- 2022;18:314-6.
15. Matsuoka S, Eguchi T, Takeda T, et al. Three-dimensional computed tomography and indocyanine green-guided technique for pulmonary sequestration surgery. *Gen Thorac Cardiovasc Surg* 2021;69:621-4.
 16. Motono N, Iwai S, Funasaki A, et al. Indocyanine green fluorescence-guided thoracoscopic pulmonary resection for intralobar pulmonary sequestration: a case report. *J Med Case Rep* 2019;13:228.
 17. Yamanashi K, Okumura N, Nakazono C, et al. Surgery for Intralobar Pulmonary Sequestration Using Indocyanine Green Fluorescence Navigation: A Case Report. *Semin Thorac Cardiovasc Surg* 2018;30:122-4.
 18. Sakuma T, Sugita M, Sagawa M, et al. Video-assisted thoracoscopic wedge resection for pulmonary sequestration. *Ann Thorac Surg* 2004;78:1844-5.
 19. Luján M, Bosque M, Mirapeix RM, et al. Late-onset congenital cystic adenomatoid malformation of the lung. Embryology, clinical symptomatology, diagnostic procedures, therapeutic approach and clinical follow-up. *Respiration* 2002;69:148-54.
 20. Nakanishi K, Kuroda H, Nakada T, et al. Thoracoscopic lobectomy using indocyanine green fluorescence to detect the interlobar fissure in a patient with displaced B3 and absence of fissure: A case report. *Thorac Cancer* 2019;10:1654-6.
 21. Obana A, Miki T, Hayashi K, et al. Survey of complications of indocyanine green angiography in Japan. *Am J Ophthalmol* 1994;118:749-53.

Cite this article as: Nakanishi K, Kadomatsu Y, Ueno H, Kato T, Nakamura S, Mizuno T, Chen-Yoshikawa TF. Complete visualization using indocyanine green in thoracic surgery for pulmonary sequestration. *J Thorac Dis* 2023;15(10):5714-5722. doi: 10.21037/jtd-23-892

Table S1 Comparison of clinical characteristics and surgical outcomes between patients who underwent segmentectomy with and without ICG

Characteristics	ICG group (n=6)	Non-ICG group (n=5)	P value
Age, years	56 [16–69]	34 [32–50]	0.43
Sex			1
Male	2 [33]	2 [40]	
Female	4 [67]	3 [60]	
Smoking history			1
Never-smoker	5 [83]	4 [80]	
Ex-smoker	1 [17]	1 [20]	
Brinkman index	0 [0–600]	0 [0–160]	1
History of pneumonia	2 [33]	2 [40]	1
Location			1
RLL	3 [50]	2 [40]	
LLL	3 [50]	3 [60]	
Size of disease, mm	45 [25–49]	36 [27–67]	1
Approach of operation			0.015
Open	1 [17]	5 [100]	
VATS	5 [83]	0	
Preoperative intervention	2 [33]	0	0.46
Operative time, min	144 [88–167]	179 [90–218]	0.43
Blood loss, mL	5 [1–191]	23 [17–116]	0.25
Postoperative hospital stays, days	5 [3–7]	10 [5–11]	0.03

Data are presented as n [%] or median [range]. ICG, indocyanine green; RLL, right lower lobe; LLL, left lower lobe; VATS, video-assisted thoracic surgery.